Heat Mass Transfer (2016) 52:671–681
DOI 10.1007/s00231-015-1587-2

ORIGINAL

Computational modeling of thermodynamic irreversibilities in turbulent non-premixed combustion

Fethi Bouras[1,2] · **Fouad Khaldi**[1]

Received: 2 April 2013 / Accepted: 4 May 2015 / Published online: 10 May 2015

Abstract This work is focused on the analysis of various computed terms of entropy generation rate in the gaseous combustion processes at different inlet temperatures of air and CH_4. Therefore, the expression of the entropy generation rate includes the effect of the viscosity friction, the thermal diffusion, the species diffusion and the chemical reaction. The expressions have been used for each term of entropy generation in order to examine the influence of each one in the overall system.

List of symbols

A	Pre-exponential factor
C	Constant models
D	Coefficient of diffusion
E	Energy activation in Arrhenius law, emperical constant in logathimic law
G	Generation of turbulent kinetic energy
g	Gravitational acceleration
h	Enthalpy
k	Kinetic turbulent energy
L	Length of combustion chamber
M	Mass molar of chemical species
p	Pressure
Q, q	Thermal heat losses, heat flux vector
R	Constant of ideal gas
R, r	Ray
S, s	Entropy, entropy source term
T	Temperature
t	Time
U, u	Axial velocity; velocity vector component; friction velocity
V	Velocity
x	Cartesian coordinate
y	Mass fraction of chemical species; distance from the wall
Y_k	Mass diffusion vector

Greeks

α	Thermal diffusivity
β	Temperature exponent
μ	Chemical potential, viscosity
ρ	Density
ε	Dissipation of energy
δ	Kronecker delta
ω	Formation rate of species in Arrhenius law
λ	Thermal conductivity
τ	Shear stress tensor
σ	Turbulent Prandtl–Schmidt number
γ	Stochometric coefficient
κ	Von Kármán constant

Indices

ch	Chemical reaction
d	Species diffusion
eff	Effective
f	Viscosity friction
gen	Generation
h	Thermal heat diffusion
i	Composite of Cartesian coordinate
in	Inlet
j	Composite of Cartesian coordinate
k	Chemical species

✉ Fethi Bouras
f.bouras@hotmail.fr

[1] LPEA, Department of Physics, Faculty of Sciences, University of HL-Batna, 05000 Batna, Algeria

[2] Department of Physics, Faculty of Sciences, University of El Oued, 039000 El Oued, Algeria

N	Number of chemical species
Out	Outlet
p	Point
t	Turbulence
w	Wall

Abbreviations

CFD	Computational fluid dynamic
UDM	User define memory

1 Introduction

The progress in industrial energy systems imposes to designers to develop more efficient systems based on particular thermodynamic approaches [1, 2]. Hereby, the final target is to minimize the thermodynamic irreversibilities occurring during the thermodynamic processes or transformations [3, 4]. It is recognized that the exergy analysis is a powerful tool for the whole thermodynamic evaluation [5–8]. Moreover, many studies investigated the fundamental methods of development of entropy generation equations to give a simplified form containing the basic variables (velocity, temperature, mass fraction…). For example, the use of the economic energy requires exploiting the theatrical models and technical process in order to reduce the energy losses and provide the maximum of power in the energy systems [8–13]. Insofar, it is shown that the geometric configuration and the topology of the system spring out of the notion of the thermodynamic irreversibilities, which is a fundamental subject of the thermodynamic optimization. That is not based only on engineering systems but also on agriculture and biology [14–16].

Stanciu et al. [17–19] considered the irreversibilities in the second law of thermodynamics to analyze both the laminar and the turbulent diffusion flame. The analysis method based on the determination of the different sources of entropy generation in the non-premixed combustion. For laminar case, the volumetric entropy generation rate expression includes the viscous friction, thermal diffusion, species diffusion and chemical reaction. Their expressions show that the corresponding irreversibilities are uncoupled if the combustion process occurs at constant a pressure. In the turbulent combustion the chemical reaction and thermal diffusion have major role in irreversibilities, comparatively to other source of combustion processes. Yapici et al. [20–23] consider the effect of oxygen percentage on the methane combustion in cylindrical combustor, in order to evaluate the local entropy generation rate due to the high temperature and velocity gradients occur the combustion and examined the various oxygen percentages using Fluent CFD code, the resulting local entropy generation rates based only on the heat transfer and the viscous friction. Accordingly, they showed that the increase of the equivalence ratio significantly reduces the entropy generation rate levels, while the total entropy generation rate decreases exponentially and the merit numbers increase. Som and Datta investigated the thermodynamic irreversibilities using the exergy destruction analysis, based on thermodynamic irreversibility in the gaseous combustion in coaxial jets confined by cylindrical combustor [7, 24]. Therefore, the authors considered the preheating of air and changing the inlet air velocity to keep the entropy generation in a combustion process, within a reasonable limit and to reduce the irreversibility in heat conduction through proper control of physical processes and chemical reactions. It has been recognized that, in almost all situations, the major source of irreversibilities is the internal thermal energy exchange associated with high temperature gradients caused by heat release in combustion reactions [7, 24]. In order to define the optimum operating condition in reactive systems, it can be determined from the parametric studies with operating parameters in different inlet conditions of the fuel and air. Moreover, the investigation in the thermodynamic irreversibilities for burner fueled by hydrogen was the objective of some studies [10, 25–27]. Where, the effects of the equivalence ratio and the inlet Reynolds number on entropy generation are studied by numerical evaluating the entropy generation equation. Therefore, the total entropy generation number can be approximated as a linear increasing function of the equivalence ratio and the inlet Reynolds number. However, its applications rely upon mitigation of heat losses which adversely affect flame stability and performance. Thereby, heat losses in turn depend upon wall properties, especially thermal conductivity. The chemical reaction, heat conduction, and mass diffusion were the dominant contributors to entropy generation in the decreasing order. So, irreversibilities due to combustion decreased as the thermal conductivities increased. Diffusion contributions were most sensitive to the changes in the thermal conductivity but chemical reaction and heat conduction contributions changed marginally [26–28].

The present paper is dealing in calculating entropy generation rate associated with the combustion of turbulent non-premixed methane/air flames in a coaxial burner. Firstly, the work is based on the validation of this study with experimental referenced data, [32], of axial velocity, temperature and mass fraction of carbon monoxide (*CO*) in some region of combustion chamber. After that, we exploit the preview results to predict the different entropy generation sources in combustion process. Finally, the behavior of each source of the entropy generation has been controlled, considering the preheating of inlet air or methane without changing the inlet rate masse flow. In order to solve the modeling equations obtained in this study, we selected

FLUENT-CFD and integrated entropy generation function in C++ language using UDMs.

2 Combustion, entropy generation concepts

The concept of combustion gives arises to use the coupling phenomenon presented in aerothermochemistry equations in order to define the characteristic parameters. In the following, we give the set of equations which define the steady combustion [7, 17–19, 25–27]:

Continuity:

$$\frac{\partial}{\partial x_i}(\rho u_i) = 0 \tag{1}$$

Momentum conservation equation:

$$\frac{\partial}{\partial x_i}(\rho u_i u_j) = -\frac{\partial p}{\partial x_i} + \frac{\partial \tau_{ij}}{\partial xj} + \rho\left(\sum_{k=1}^{n} y_k g_{ki}\right) \tag{2a}$$

The viscous stress tensor can write in turbulent flows:

$$\tau_{ij} = \bar{\tau}_{ij} + \tau_{ij,t} \tag{2b}$$

$\bar{\tau}_{ij}$: Mean stress tensor, $\tau_{ij,t}$: Turbulent stress tensor.

And,

$$\bar{\tau}_{ij} = \mu\left[\frac{\partial \bar{u}_i}{\partial x_j} + \frac{\partial \bar{u}_j}{\partial x_i} - \frac{2}{3}\delta_{ij}\frac{\partial \bar{u}_l}{\partial x_l}\right] \tag{2c}$$

$$\tau_{ij,t} = -\overline{\rho u_i'' u_j''} \tag{2d}$$

Energy conservation equation

$$\frac{\partial}{\partial x_i}(\rho u_i h) = u_i\frac{\partial p}{\partial x_i} + \tau_{ij}\frac{\partial u_i}{\partial x_j} - \frac{\partial q_i}{\partial x_i} - \frac{\partial}{\partial x_i}\left(\sum_{k=1}^{n}\rho y_k U_{k,i} h_k\right) + \rho\sum_{k=1}^{n} y_k f_{k,i} U_{k,j} \tag{3a}$$

In turbulent combustion case the heat transfer flux can given as:

$$q_i = \bar{q}_i + q_{i,t} \tag{3b}$$

$\bar{q}_i$: Mean heat flux vector, $q_{i,t}$: Turbulent heat flux vector.

Where:

$$\bar{q}_i = -\lambda\frac{\partial \bar{T}}{\partial x_i} \tag{3c}$$

$$q_{i,t} = -\overline{\rho u_i'' T''} \tag{3d}$$

Mass conservation equation of individual species:

$$\frac{\partial}{\partial x_i}(\rho u_i y_k) = -\frac{\partial Y_k}{\partial x_i} + \dot{\omega}_k \tag{4a}$$

Mass diffusion vector for the turbulent combustion is expressed by:

$$Y_k = \bar{Y}_k + Y_{k,t} \tag{4b}$$

$\bar{Y}_k$: Mean mass diffusion vector, $Y_{k,t}$: Turbulent mass diffusion vector.

In which:

$$\overline{Y}_k = -\frac{\partial \bar{\rho} D_k \bar{y}_k}{\partial x_i} \tag{4c}$$

$$Y_{k,t} = -\overline{\rho u_i'' y_k''} \tag{4d}$$

Thermodynamic status

$$p = \rho RT\sum_{k=1}^{n}\frac{y_i}{M_i} \tag{5}$$

Turbulence kinetic energy:

$$\frac{\partial}{\partial x_i}(\rho u_i k) = \frac{\partial}{\partial x_j}\left(\mu + \frac{\mu_t}{\sigma_k}\right)\frac{\partial k}{\partial x_j} + G_k - \rho\varepsilon + S_k, \tag{6}$$

Dissipation rate:

$$\frac{\partial}{\partial x_i}(\rho u_i \varepsilon) = \frac{\partial}{\partial x_j}\left(\mu + \frac{\mu_t}{\sigma_\varepsilon}\right)\frac{\partial \varepsilon}{\partial x_i} + C_{1\varepsilon}\frac{\varepsilon}{k}G_\varepsilon - C_{2\varepsilon}\rho\frac{\varepsilon}{k} + S_\varepsilon. \tag{7}$$

where $C_{1\varepsilon} = 1.44$, $C_{2\varepsilon} = 1.92$, $\sigma_k = 1.0$, $\sigma_\varepsilon = 1.3$

The combustion reaction is modeled with a two-steps reaction mechanism where the production and the combustion of carbon monoxide (CO) are taken into account. In the first stage, methane is oxidized into carbon monoxide and water vapor, but in the second, carbon monoxide is oxidized into carbon dioxide. The reaction mechanism takes place according to the constraints of chemistry, and is defined by stoichiometric equation [7, 17, 22, 23]:

Reaction 1:

$$CH_4 + \frac{3}{2}O_2 \rightarrow CO + 2H_2O \quad \text{(step 1)} \tag{8a}$$

Reaction 2:

$$CO + \frac{1}{2}O_2 \rightarrow CO_2 \quad \text{(step 2)} \tag{8b}$$

Once the computations achieved the results obtained will be exploited to calculate the local entropy generation rate [7, 13, 19, 26]:

$$\dot{S}_{gen} = \left(\dot{S}_{gen}\right)_f + \left(\dot{S}_{gen}\right)_h + \left(\dot{S}_{gen}\right)_d + \left(\dot{S}_{gen}\right)_{ch} \tag{9}$$

where $\left(\dot{S}_{gen}\right)_f$: Volumetric entropy generation rate by fluid friction,

$$\left(\dot{S}_{gen}\right)_f = \frac{\mu_{eff}}{T}\frac{\partial u_i}{\partial x_j}\frac{\partial u_i}{\partial x_j} > 0 \tag{10}$$

$\left(\dot{S}_{gen}\right)_h$: Volumetric entropy generation rate by heat transfer,

$$\left(\dot{S}_{gen}\right)_h = \frac{\lambda_{eff}}{T^2}\frac{\partial T}{\partial x_j}\frac{\partial T}{\partial x_j} > 0 \tag{11}$$

$\left(\dot{S}_{gen}\right)_d$: Volumetric entropy generation rate by diffusion of species,

$$\left(\dot{S}_{gen}\right)_d = \sum_{k=1}^{n} \rho D_k \frac{R_k}{y_k}\frac{\partial y_k}{\partial x_i}\frac{\partial y_k}{\partial x_i} > 0, \tag{12}$$

$\left(\dot{S}_{gen}\right)_{ch}$: Volumetric entropy generation rate by chemical reaction,

$$\left(\dot{S}_{gen}\right)_{ch} = \frac{\dot{\omega}}{T}\sum_{k=1}^{n}(\gamma_k' - \gamma_k'')\mu_k > 0, \tag{13}$$

And;

$$\mu_k = h_k - T_0 s_k, \tag{14}$$

Using Arrhenius law for the reaction of two steps, the Eq. (13) becomes,

$$\left(\dot{S}_{gen}\right)_{ch} = \left(\dot{S}_{gen}\right)_{ch,1} + \left(\dot{S}_{gen}\right)_{ch,2}, \tag{15}$$

$$\left(\dot{S}_{gen}\right)_{ch;1} = \frac{\dot{\omega}_1}{T}\sum_{k=1}^{n}\left(\gamma_{k,1}' - \gamma_{k,1}''\right)\mu_{k,1} > 0, \tag{16a}$$

$$\left(\dot{S}_{gen}\right)_{ch;2} = \frac{\dot{\omega}_2}{T}\sum_{k=1}^{n}\left(\gamma_{k,2}' - \gamma_{k,2}''\right)\mu_{k,2} > 0, \tag{16b}$$

In order to compute the forward constant rate related to reactions, we consider the expanded version of the Arrhenius expression:

$$\dot{\omega} = AT^{\beta}e^{-\frac{E}{RT}} \tag{17a}$$

where A: Pre-exponential factor; E: Activation energy; R = 8313 J/kgmol; K: Universal gas constant; T: Temperature; β: Temperature exponent.

Based on many studies, [29–31], focused on the same configuration (type of fuel, cylindrical burner and turbulent combustion) we have considered that β = 0. Hereby, the Arrhenius law is given in the simple form:

$$\dot{\omega} = Ae^{-\frac{E}{RT}} \tag{17b}$$

The near solid boundary modeling has an impacts on the numerical solutions. The standard wall functions in FLUENT-CFD are focused on the proposal of Launder and Spalding, and have been most extensively used in the similar study of current investigation. Where, the wall law for the mean velocity is given by:

$$U^+ = \frac{1}{\kappa}\ln\left(Ey^+\right) \tag{18a}$$

$$U^+ = \frac{U_p C_\mu^{1/4} k_p^{1/2}}{\tau_w/\rho} \tag{18b}$$

$$y^+ = \frac{\rho C_\mu^{1/4} k_p^{1/2} y_p}{\mu} \tag{18c}$$

where $\kappa = 0.4187$: Von Kármán constant; $E = 9.793$: Emperical constant; U_p: Mean velocity of the fluid at point p; k_p: Turbulence kinetic energy at point p; y_p: Distance from point p to the wall; μ: Dynamic viscosity of the fluid.

In FLUENT-CFD, the wall laws for mean velocity and temperature are based on the wall unit, y^+, instead of $y^+ \equiv \rho u_\tau y/\mu$. These quantities are approximately equal in equilibrium turbulent boundary layers. And, the logarithmic law for mean velocity is validated when $30 < y^+ < 300$. Indeed, the logarithmic law is employed when $y^+ > 11.225$ in FLUENT-CFD. In Fig. 1, we illustrate the variation of y^+ for the combustion chamber wall in the current study.

In order to give the wall law for temperature, the Reynolds analogy between momentum and energy transport offer a similar logarithmic law for mean temperature. For doing so, the FLUENT-CFD calculation based on:

- Linear law for the thermal conduction sublayer where conduction is important;
- Logarithmic law for the turbulent region where effects of turbulence dominate conduction.

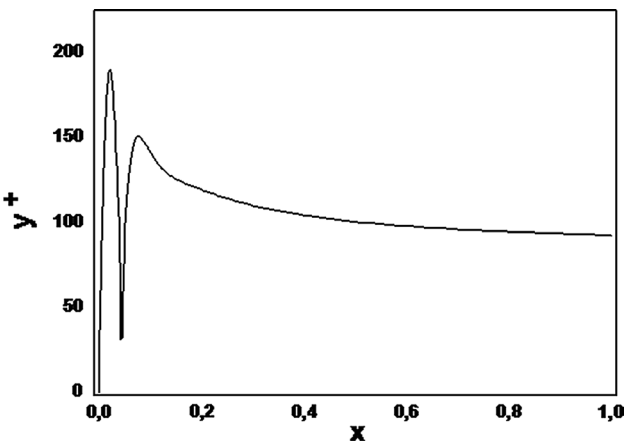

Fig. 1 Profile of y^+ for the combustion chamber wall

The thickness of the thermal conduction layer is, in general, different from the thickness of the (momentum) viscous sublayer, and changes from fluid to fluid. For example, the thickness of the thermal sublayer for a high Prandtl number fluid is much less than its momentum sublayers thickness. For fluids of low Prandtl numbers, on the contrary, it is much larger than the momentum sublayer thickness. Furthermore, the impact of the highly compressible flows on the temperature distribution in the near solid boundary region can be significantly different due to the heating by viscous dissipation. Whereof, the temperature wall functions include the contribution from the viscous heating (for more details, see FLUENT help).

3 Experimental configuration and application domain

The present study is a continuation of a previous numerical analysis [33, 34] proposed to support the experimental work [32] interested in turbulent diffusion flames characterization. The burner depicted in Fig. 2 and considered in the experimental study consists of a coaxial jets discharging into a cylindrical chamber o pressurized to 3.8 atm. The burner is of ray R4 = 0.06115 and length L = 1 m and is with isothermal walls of 500 K. The fuel (CH4) is issued from the inner jet with ray R1 = 0.03157 m, with the velocity of 0.987 m/s at temperature of 300 K, while the preheated air at temperature T2 = 750 K is supplied from the annular jet of external ray R3 = 0.04685 m at a velocity of 20.63 m/s.

The present study investigates two dimensions (2D) numerical modeling of the entropy generation of non-premixed turbulent combustion. We performed the geometry and meshes depicted in Fig. 3 by GAMBIT, and the chosen meshes are of quadrilateral type, where the selected grid is smoothed in region nearby to the solid walls of burner and in the level of interaction of air and CH_4, in order to accommodate more information in solid boundary and flame zone. The volume contains approximately 40.000 cells, the size of a cell ranges from 4.87e−09 to 1.52e−04 m^2.

4 Results and discussion

All calculations are carried out by FLUENT-CFD to resolve the governing equations mentioned previously. We note that the SIMPLEC algorithm is used for pressure velocity coupling. And, the convergence criteria for solving equations are equal to 10^{-3}. In this part of work we illustrate two kinds of results. The first one is the validation of computational profiles of axial velocity, temperature field and carbon monoxide mass fraction with experimental data for methane fueled coaxial jet combustor [32–34]. And the second one, previously obtained results are exploited to evaluate the entropy generation for different cases of flows.

4.1 Numerical validation

The primary quantities were tested against experimental data that are used the length R and the velocity U

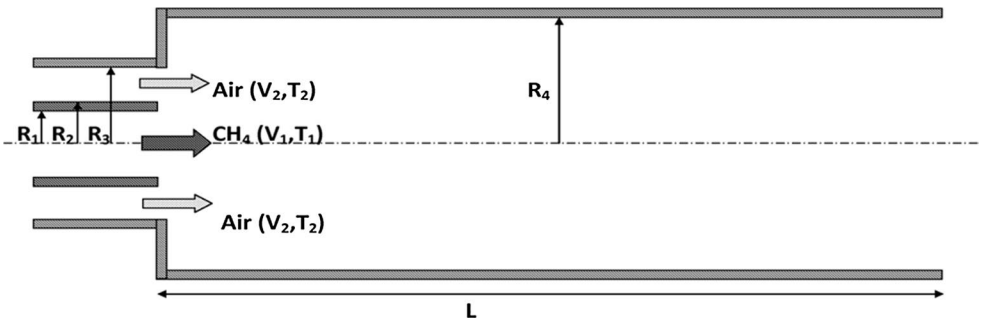

Fig. 2 Schematic of the combustion chamber

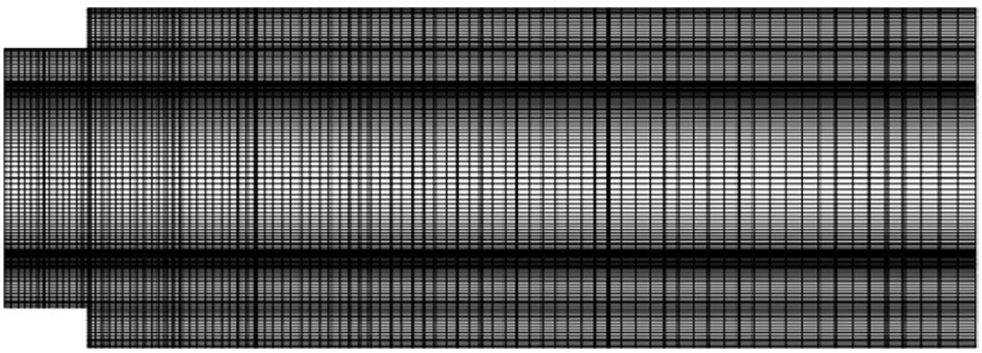

Fig. 3 Computational domain and the grid used in the simulation

normalized by the injector radius (R ≡ R3) and the inlet bulk velocity of the air (U ≡ V2).

4.1.1 Axial velocity

Figure 4 present the comparison of computational and experimental radial profile of axial velocity. Indeed, the velocity fields achieve significantly better agreement with the experiment at two measurement stations *x/R = 0.14* and *x/R = 4.67*. The mean axial velocity ranges from about *u/U = −0.15–1.1*, where the maximum is located the flame zone. The negative values of velocity are present close to the wall in the recirculating region and in a bluff body in the center of burner: a brutal variation of in the section of the burner results the creation of the recirculating zones what can be explained by the significant negative values observed close to the wall. In addition, the difference between the inlet velocity of CH_4 and air produce the second zone of recirculation, it appeared in the center of the combustion chamber. The meeting of the two inlet flows characterized by high mixture level generated by the shearing where the flame stabilized in this region [17, 32–34]. The zone of the flame is the seat of the great values of velocity. In particular, the position of peak velocity is reproduced well by the present numerical computation. Furthermore, in the recirculating region and the flame holder, the agreement is satisfactory.

4.1.2 Temperature

The comparisons of the predicted radial profiles of temperature with those of experiments at two measurement stations, x/R = 4.52 and x/R = 5.20, are shown in Fig. 5.

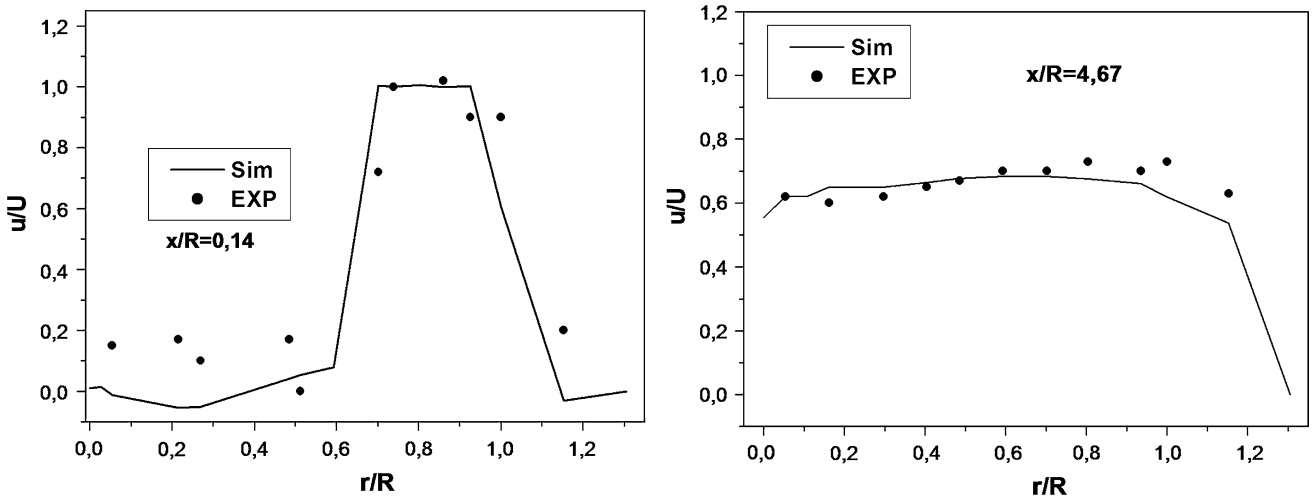

Fig. 4 Radial profiles of normalized axial velocity

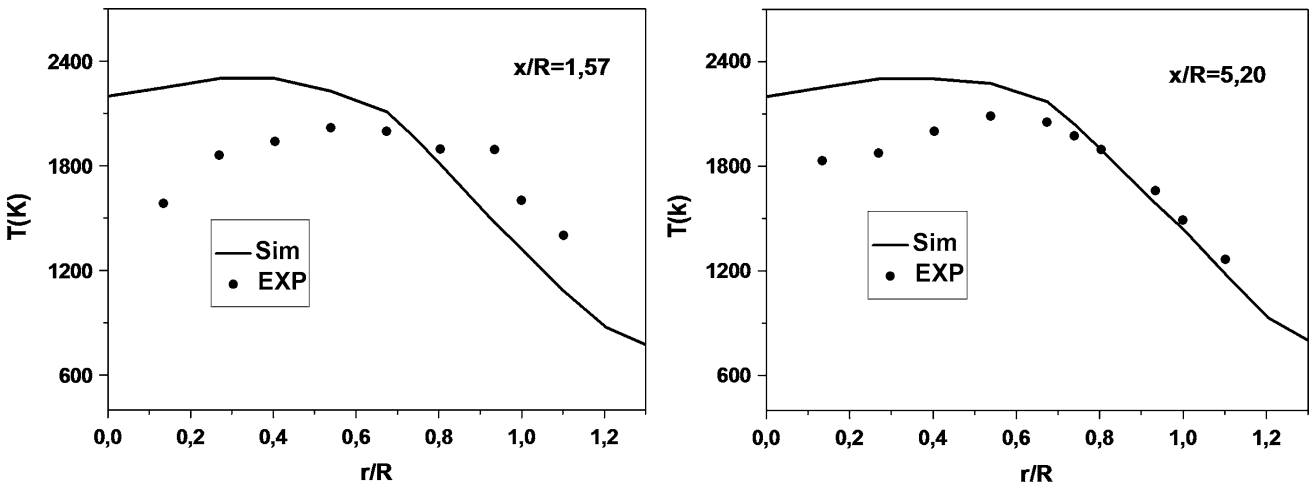

Fig. 5 Radial profiles of Temperature

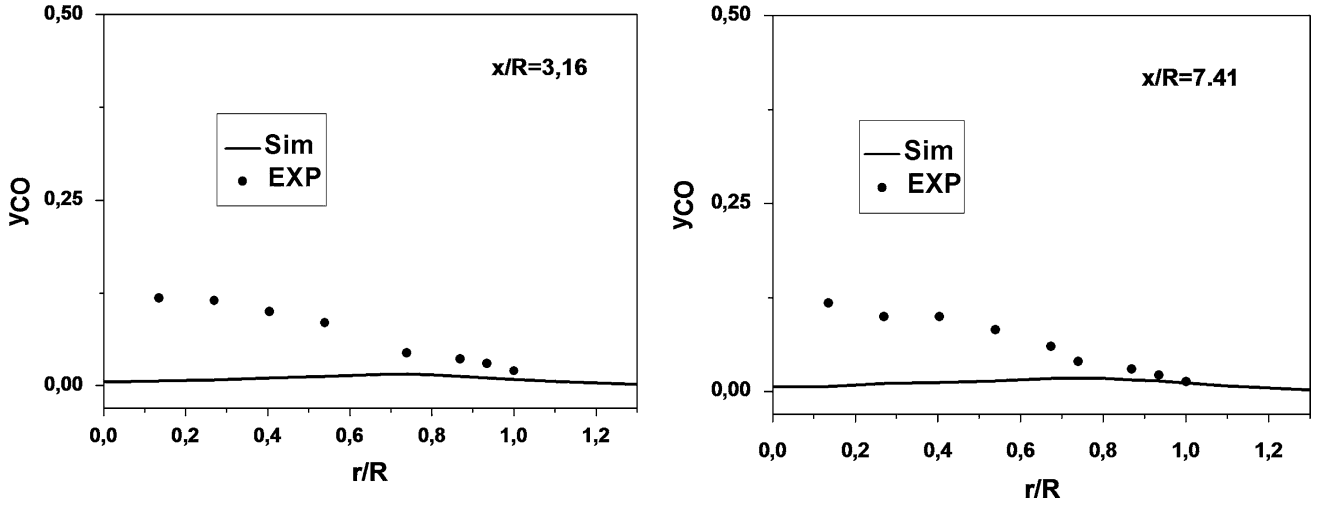

Fig. 6 Radial profiles of carbon monoxide mass fraction

Temperature is a quantity that is derived from the energy equation by assuming isothermal walls and neglecting thermal radiation. The high values of the temperature are located within the reaction zone around the center of burner; away the temperature decreases to achieve the wall temperature. Indeed, the numerical temperature profiles give similar experimental trends but with overestimation, especially near the center of the burner. The expected overprediction of temperature can be attributed to three factors: (1) ignoring of thermal radiation by the numerical simulation, (2) experimental uncertainty, especially in regions with large temperature fluctuations, and (3) difficulty to ensure perfectly the experiment condition of isothermal water-cooled walls at 500 K [24, 26].

4.1.3 Carbon monoxide mass fraction

The solution of mass fraction of species equations (CH_4, O_2, CO, CO_2 and H_2O) are founded on Arrhenius law, in order to estimate production or consumption of each species considered in the reaction. The discussion of the numerical calculation validity concerning the species concentrations fields is based on plotting the radial evolution of the mass fraction of CO, predicted as well as measured, at two measurement stations, x/R = 0.14 and x/R = 4.67, see Fig. 6. At both reference points, there are some shifts near the center of the burner, in other word around the flame front. The measurements reveal that the CO concentration decreases more brutally when going away the center of the burner, than what the computations predicate. This relative difference can be attributed to the limitation of the chemical mechanisms, two steps exothermic reactions, chosen for modeling the combustion reaction. More developed chemical model should give better results in regard to species concentrations [32, 34].

4.2 Entropy generation analysis

Figure 7 illustrates the pie chart of the entropy generation rate due to viscosity friction, heat transfer (thermal diffusion), mass diffusion and chemical reaction. This is for the non-premixed combustion in the confined domain (combustion chamber) for the reference flow case. The entropy

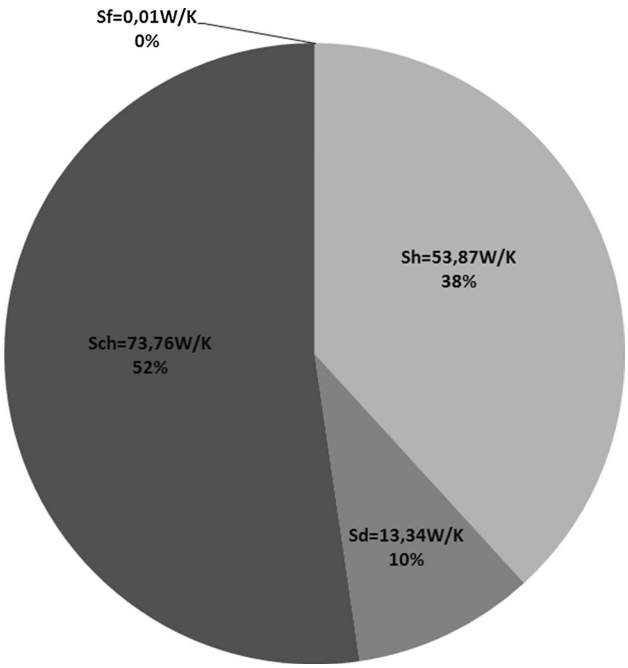

Fig. 7 Pie chart of entropy generation sources for the reference flow case

generation rate due to the chemical reaction is greater than that due to the heat diffusion. Moreover, the entropy generation due to the chemical reaction is a much greater compared to the entropy generated by species diffusion. However, the entropy generation due to friction viscosity is significantly neglected compared to the other sources of entropy generation. Therefore, high diffusion of heat continues over a much larger volume to cause a high overall entropy generation due to thermal diffusion (38 %). The great values of entropy production are due to the chemical reaction, 52 %, mainly around the flame. The contribution of entropy generation due to the species diffusion is equal to 10 % which is in low effect comparatively to the thermal and chemical reaction.

Figure 8 show the radial profiles of the volumetric entropy generation rate by different mechanisms for the same two stations in combustor. The height values of entropy generation are due to friction, Fig. 8a, presented in the zones of shearing where the two flows of CH_4 and Air are meeting and in the zones near to the wall. Therefore, those zones are characterized by a strong gradient of velocity. In first station ($x/R = 3.16$), Fig. 8a, the two peaks are well reproduced. However, in second station, $x/R = 7.41$, the peaks are disappeared, which means that this station is far from the shear zone, though we consider that the peak nears the side is still generated by the walls. Figure 8b shows the radial variation of the thermal diffusion volumetric entropy generation which is due to the combustion process and isothermal walls of the burner. The high values of the temperature gradient localized in the flame region. So, the use of the Eq. (11) to evaluate the volumetric entropy generation gives the high values of the thermal diffusion in the flame region, where the gradient of temperature is higher [7, 12, 26]. Moreover, the gradient of the fuel concentration is higher in the flame zone, which is the zone of reaction. Accordingly, the fuel and the air are consumed in order to produce CO_2, CO and H_2O; the behavior of the volumetric entropy generation caused by diffusion species and volumetric entropy generation due to chemical reaction are the same (Fig. 8c, d). Therefore, the gradient of the mass fraction gives the considerable values in the flame zone. Consequently, the entropy generation is due to the thermal diffusion, the entropy generation is due to the species diffusion and the entropy generation produced by the

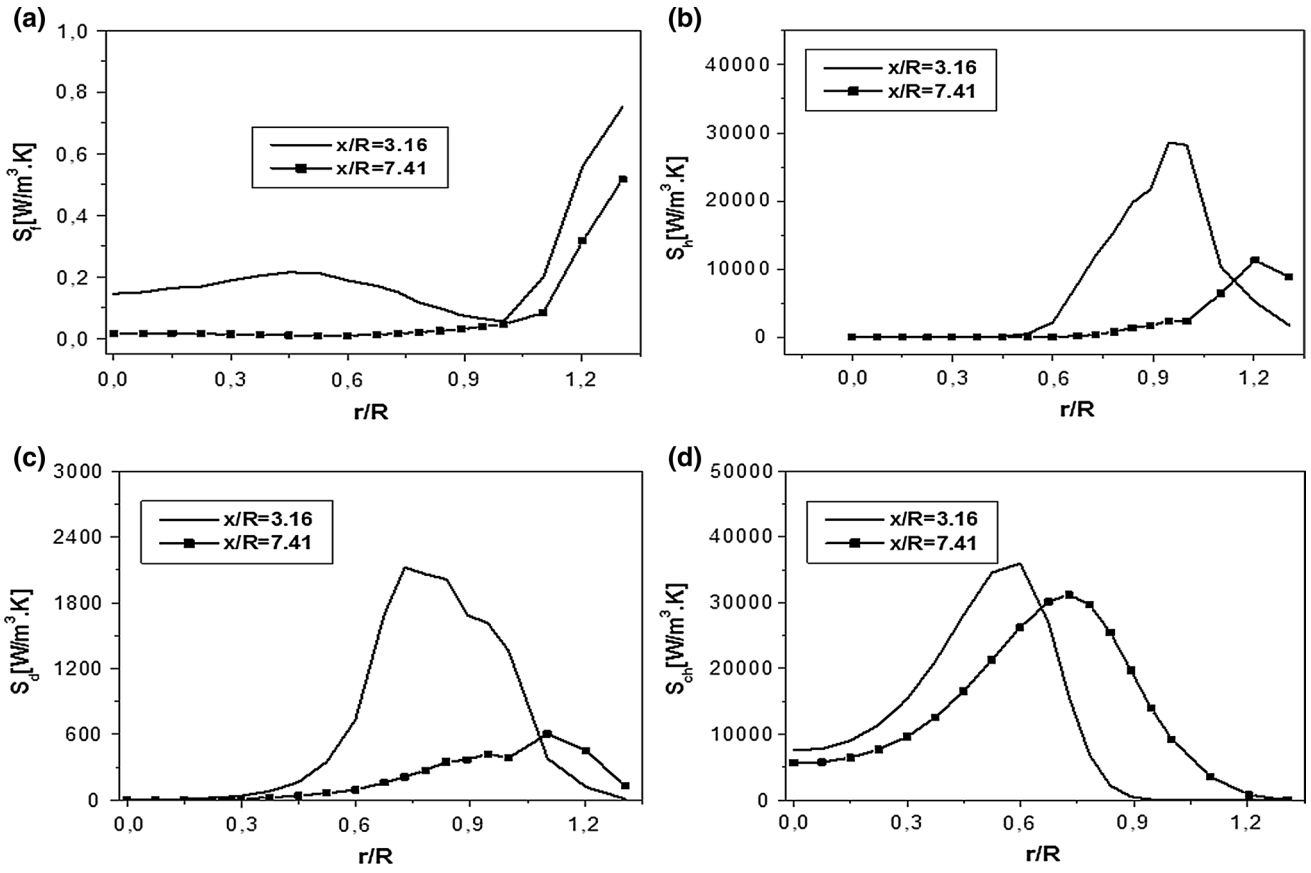

Fig. 8 Radial variation of volumetric entropy generation: **a** entropy generation due to the viscosity friction; **b** entropy generation due to the thermal diffusion; **c** entropy generation due to the species diffusion; **d** entropy generation due to the chemical reaction

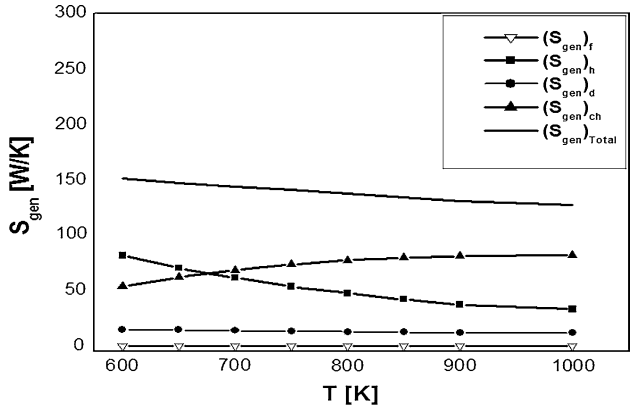

Fig. 9 Effect of preheating the inlet air on entropy generation sources

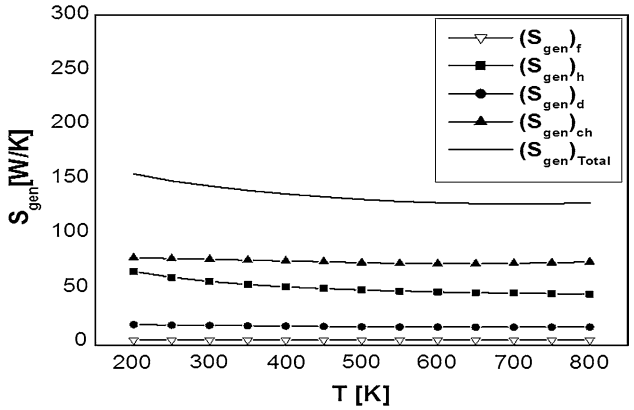

Fig. 10 Effect of preheating the inlet CH_4 on entropy generation sources

chemical reaction, give the same tendency (Fig. 8b, c, d) because the combustion encounters all those phenomenon where they take place within the flame front [17–19].

4.2.1 Preheating of air

The obtained values of the total entropy generation using detailed method to calculate each term based on the Eqs. (9–17). The effect of preheated air on entropy generation showed, Fig. 9, which the total rate of entropy generation decreases with the increase in the inlet air temperature. The variation is principally attributed to the decrease in the contributions of all entropy generation terms with the preheated air in a stoichiometric CH_4—air flame which gives a reduction in the total entropy generation of 0.5 % with the difference of 10 °C of temperature relatively to reference flow case. Moreover, approximately the entropy generation due to the thermal diffusion is lower by 27. 32 %, for the species diffusion reduced by 24.28 % and the contribution of chemical terms minimized by 4.39 % comparatively to the reference flow. However, the effect of the preheated air was on the entropy generation due to the viscosity friction is negligible comparatively to other terms of the total entropy generation. The higher value of air temperature decreases the temperature gradient occurring in most of the region of the domain resulting in a reduction in the diffusive heat flux. So, that caused the low of the entropy generation due to the thermal diffusion. The combustion reaction was assumed to be complete and the product concentrations were calculated from chemical equilibrium consideration at a high temperature. The higher initial temperature of the reactant decreases the entropy generation in the combustion process due to the higher temperature of the product, which retains more entropy contained in it. Thus, the entropy generation per unit mass of the fuel increased as the reactant mixture became leaner than stoichiometric. This may be attributed to the lower temperature of the flame in a lean mixture and the inherent irreversibility associated with the mixing of the combustion products with the excess air presented in the combustor. Finally, we observed that in the non-premixed combustion the reactant temperature should be kept higher to ensure less entropy generation.

4.2.2 Preheating of fuel

In this part of work we performed a detailed numerical analysis for the study of entropy generation considering the preheated CH_4 at the inlet using the mathematical equations presented previously (9–17). Figure 10 illustrates the obtained entropy generation sources rates at different CH_4 inlet temperature. It has been shown that the total rate of entropy generation becomes large in the region of high temperature gradient. The chemical reaction accounted for the maximum entropy generation in CH_4 flame, while thermal diffusion contributed in the second largest one after the entropy generation due to the chemical reaction. The contribution of diffusion species gives less impact comparatively to two previous sources. However, the effect of the viscous dissipation is negligible of the total entropy generation. Moreover, the preheated fuel in a stoichiometric, CH_4—air, flame has given a reduction in the total entropy generation approximately by 0.4 % with the difference of 10 °C of temperature relatively to the reference flow. However, the effect of the preheated fuel was found to be much smaller, and the effect of the viscous dissipation is negligible of the total entropy generation. So, that decreases with the increase of inlet temperature of fuel (CH_4).

5 Conclusion

This work is focused on the recapitulation of the fundamental notion of the entropy generation in order to realize

complete study of reactif system: aerodynamic, thermal, species and entropy generation analysis in academic configuration similar to the combustion chamber of gas turbine, and test it under different preheating inlet temperatures for air or fuel. The numerical calculations of the present investigation are carried out by FLUENT-CFD including our UDM and UDF in C++ language for total and each term of entropy generation. Then, it appears that chemical reaction and heat transfer entropy generation sources are the more important responsible of thermodynamic irreversibilities; they are responsible, respectively, by 50 and 40 % of entropy generation. The species diffusion has moderate role, around 10 %, while the irreversibilities generated by viscous friction are negligible. Preheating inlet air and CH_4 have positive impact on the total thermodynamic irreversibilities associated with the combustion processes. Finally, regarding the limitation in dynamic model ($k-\varepsilon$) and the mechanism of combustion (stoichiometric combustion, reaction two steps), so this work can be improved by including other models of turbulence considering different scales (LES or DNS) and multispecies mechanisms of combustion model (PDF) in order to establish a maximum of chemical species in reaction comparatively to the experimental case.

References

1. Vargas JVC, Bejan A (2001) Thermodynamic optimization of finned crossflow heat exchangers for aircraft environmental control systems. Int J Heat Fluid Flow 22:657–665
2. Nishida K, Takagi T, Kinoshita S (2002) Analysis of entropy generation and exergy loss during combustion. Proc Combust Inst 29:869–874
3. Ribeiro B, Martins J, Nunes A (2007) Generation of entropy in spark ignition engines. Int J Thermodyn 10:53–60
4. Durmayaza A, Salim Sogutb O, Sahinc B, Yavuz H (2004) Optimization of thermal systems based on finite-time thermodynamics and thermoeconomics. Prog Energy Combust Sci 30:175–217
5. Rosen MA (2002) Clarifying thermodynamic efficiencies and losses via exergy. Exergy Int J 2:3–5
6. Caton JA (2000) On the destruction of availability (exergy) due to combustion processes—with specific application to internal-combustion engines. Energy 25:1097–1117
7. Som SK, Datta A (2008) Thermodynamic irreversibilities and exergy balance in combustion processes. Prog Energy Combust Sci 34:351–376
8. Bejan A (2002) Fundamentals of exergy analysis, entropy generation minimization, and the generation of flow architecture. Int J Energy Res 26:545–565
9. Bejan A, Lorente S (2004) The constructal law and the thermodynamics of flow systems with configuration. Int J Heat Mass Transf 47:3203–3214
10. Rakopoulos CD, Giakoumis EG (2006) Second-law analyses applied to internal combustion engines operation. Prog Energy Combust Sci 32:2–47
11. Lior N, Sarmiento-Darkin W, Al-Sharqawi HS (2006) The exergy fields in transport processes: their calculation and use. Energy 31:553–578
12. Forland T, Ratkje DK (1980) Entropy production by heat, mass, charge transfer and specific chemical reactions. Electrochim Acta 25:157–163
13. San JY, Worek WM, Lavan Z (1987) Entropy generation in combined heat and mass transfert. Int J Heat Mass Transf 30:1359–1369
14. Shiba T, Bejan A (2001) Thermodynamic optimization of geometric structure in the counterflow heat exchanger for an environmental control system. Energy 26:493–511
15. Bejan A (1996) Method of entropy generation minimization, or modeling and optimization based on combined heat transfert and thermodynamics. Rev Cén Therm 35:637–646
16. Tatarin V, Borodiouk O (1999) Entropy calculation of reversible mixing of ideal gases shows absence of gibbs paradox. Entropy 1:25–36
17. Stanciu D, Marinescu M, Dobrovicescu A (2007) The influence of swirl angle on the irreversibilities in turbulent diffusion flames. Int J Thermodyn 10:143–153
18. Stanciu D, Isvoranu D, Marinescu M (2001) Second law analysis of diffusion flames. Int J Appl Thermodyn 4:1–18
19. Stanciu D, Marinescu M, Isvoranu D (2000) Second law analysis of the turbulent flat plate boundary layer. Int J Appl Thermodyn 3:99–104
20. Yapici H, Kayataş N, Kahraman N, Baştürk G (2005) Numerical study on local entropy generation in compressible flow through a suddenly expanding pipe. Entropy 7:38–67
21. Yapici H, Kayatas N, Albayrak B, Basturk G (2005) Numerical calculation of local entropy generation in a methane–air burner. Energy Convers Manag 46:1885–1919
22. Yapici H, Basturk G, Kayatas N, Yalcin S (2005) Numerical study on transient local entropy generation in pulsating turbulent flow through an externally heated pipe. Sadhana 30:625–648
23. Yapici H, Basturk G, Kayatas N, Albayrak B (2004) Numerical study of effect of oxygen fraction on local entropy generation in a methane–air burner. Sadhana 29:641–667
24. Datta A (2005) Effects of gravity on structure and entropy generation of confined laminar diffusion flames. Int J Therm Sci 44:429–440
25. Chen S (2010) Analysis of entropy generation in counter-flow premixed hydrogen–air combustion. Int J Hydrog Energy 35:1401–1411
26. Yapici H, Basturk G, Kayata N, Albayrak B (2006) Effect of oxygen fraction on local entropy generation in a hydrogen–air burner. Heat Mass Transfer. 43:37–53
27. Jejurkar SY, Mishra DP (2011) Effects of wall thermal conductivity on entropy generation and exergy losses in a H2-air premixed flame microcombustor. Int J Hydrog Energy 36:15851–15859
28. Daw CS, Chakravarthy K, Conklin JC, Graves RL (2006) Minimizing destruction of thermodynamic availability in hydrogen combustion. Int J Hydrog Energy 31:728–736
29. Nieckele AO, Naccache MF, Gomes MSP, Carneiro JE, Serfaty R et al (2001) Evaluation of models for combustion processes in a cylindrical furnace. In: International conference of mechanical engineering, ASME-IMECE, New York, 11–16 Nov
30. Da Silva CV, Vielmo HA, França FHR (2006) Numerical simulation of the combustion of methane and air in a cylindrical chamber. Therm Eng 5:13–21
31. Carneiro JNE, Silva BG, Nieckele AO, Naccache MF, Gomes MSP (2004) Numerical comparison of the combustion process inside an aluminum melting furnace with natural gas and liquid pentane. In: Proceedings of the 10th Brazilian congress of thermal sciences and engineering-ENCIT 2004. Rio de Janeiro, Brazil, 29 Nov–03 Dec
32. Pierce CD, Moin P (2004) Progress-variable approach for large-eddy simulation of non-premixed turbulent combustion. J Fluid Mech 504:73–97

33. Bouras F, Soudani A, Si Ameur M (2010) Beta-pdf approach for large-eddy simulation of non-premixed turbulent combustion. Int Rev Mech Eng 4:358–363

34. Bouras F, Soudani A, Si Ameur M (2012) Thermochemistry study of internal combustion engine. Energy Procedia 18:1086–1095